Carbohydrate Research, 78 (1980) 89–109

HELICAL PARAMETERS OF INFINITE POLYMER CHAINS HAVING A DIAMOND-LIKE BACKBONE. APPLICATION TO HOMOPOLYSACCHARIDES AND CYCLIC OLIGOSACCHARIDES

DIDIER GAGNAIRE, SERGE PÉREZ,
Centre de Recherches sur les Macromolécules Végétales, (CNRS) 53 X, 38041 Grenoble cédex (France)
AND VINH TRAN
Département de Recherche Fondamentale. Laboratoire de Chimie Organique Physique. Centre d'Études Nucléaires, 85X, 38041 Grenoble cédex (France)
(Received October 17th, 1978; accepted for publication in revised form, February 20th, 1979)

ABSTRACT

Helical conformations of infinite polymer chains may be described by two helical parameters: n and h. General n,h maps have been produced that are independent of the monomer chemistry, except for the limitation of tetrahedral geometry. Some very simple geometrical criteria have been found to underlie the general aspects of the maps obtained. These maps are found to cover the whole range of predictable secondary structures of homopolysaccharides having the (1→2), (1→3), and (1→4) linkage-types. Moreover, a general strategy for investigating the secondary structures of (1→6)-linked homopolysaccharides is proposed. In an extension of these results, the prediction of the possibility of a stable cyclic tetrasaccharide made up of (1→6)-β-D-glucose residues, is proposed and analyzed.

INTRODUCTION

Among the different types of information provided by an X-ray fiber diffraction-pattern, one of the most "potent" is obtained on the meridian of the diagram, namely, the fiber repeat and the symmetry of the polymeric backbone. This represents a fundamental set of molecular parameters, as the values are directly related to the relative arrangement of contiguous repeating-units. The relative orientation of two linked units may be specified by the dihedral angles at the given linkage. When these dihedral angles are the same at every linkage, the polymer adopts a regular, helical conformation. Such a helical arrangement is customarily described in terms of a set of helical parameters: (n,h), n being the number of residues per turn of the helix, and h being the translation of the corresponding residue along the axis of the helix.

The helical parameters (n,h) of regular conformations may be calculated directly from a set of internal coordinates (incorporating the bond lengths, bond angles, and dihedral angles) by means of equations derived by Miyazawa[1] and Sugeta and Miyazawa[2,3]. Theoretically, these equations should have permitted these

operations to be performed in two ways. In one way, with the values of all of the internal coordinates being known, n and h are computed. In the other way, n and h are specified, and helical structures are generated consistent with these values. Whereas the first operation is trivial, the latter one is far from obvious. To the best of our knowledge, it has only been applied to the simple case of polypeptides[4]. In fact, the latter option is usually performed graphically. The helical parameters n and h are plotted as *iso-n* and *iso-h* contours on the same map, as a function of variable dihedral-angles. The values of the variable torsion-angles generating helical structures consistent with given set of helical parameters are found at the intersections of the corresponding *iso-n* and *iso-h* contours. An alternative graphical method, that of rotation of the residue about a virtual bond, has also been elaborated[5,6].

Although it has long been recognized that helices comprise the single, most important, secondary structural form, little has been done to clarify the geometrical criteria underlying the aspects of the n,h maps obtained. In an attempt to do so, we have undertaken a general study of n,h maps that are independent of monomer chemistry except for the limitation of tetrahedral geometry. Beside the interest that the elucidation of such geometrical criteria would have, the series of n,h maps obtained is well suited for use in the investigation of a broad number of polymers. To illustrate such an application, homopolysaccharides, for which some of helical maps have already be given[7-9], have been selected.

METHOD OF CALCULATIONS

Helical parameters were evaluated by the method of Miyazawa[1]. In keeping with the basic idea of expressing the helical parameters as functions of internal parameters, namely, bond lengths, bond angles, and torsion angles (Fig. 1), an algorithm, expressed in a binary representation[10], was used. Such a general method allows calculation of helical parameters for any polymer chain made up of i atoms. All of the following examples and associated maps were computed and drawn by using a Hewlett–Packard 9825 calculator connected to a 9872A plotter*.

In order to keep with a readily visualized representation, the question was restricted to a two-dimensional problem, namely, two variable torsional angles θ_1 and θ_2, within a repeat-unit made up of i atoms. In this method, the $(i-2)$ torsion angles and all of the i bond lengths and bond angles are kept invariant, and all possible chain conformations are created by stepping through $-180°$ to $180°$ about the variable bonds (θ_1 and θ_2 rotations) at suitable intervals (usually 10°). A further restriction arises from the fact that the variable torsion-angles θ_1 and θ_2 were deliberately chosen as contiguous along the polymeric backbone. Hence, the repeating unit is simply defined by θ_1/sequence/θ_2. Within these limits, and for $1 \leqslant (i-2) \leqslant 3$, all of the conformations of the sequence arising from the different combinations of torsion angles existing in a *trans* (T) and/or perfectly *gauche*$^+$ (G^+) and *gauche*$^-$

*A Hewlett–Packard programming-system version of the program is available from the authors.

(G^-) forms were generated. The sign of the angles is defined according to the rules recommended by the IUPAC–IUB Commission of Biochemical Nomenclature[11]. In order to assign the bond lengths given, bond angles, and the different combinations of T, G^+, and G^- conformations, a diamond-lattice representation was used. All of the bond lengths were given values of 1.54 Å, and the bond angles were assigned a

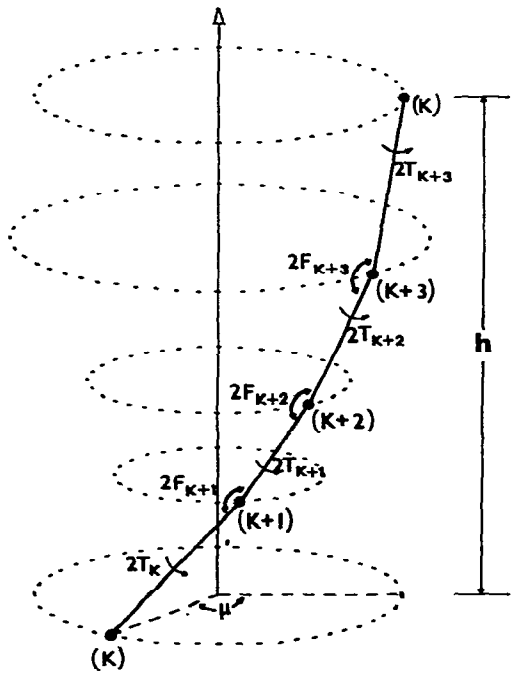

Fig. 1. Schematic diagram of the internal coordinates: R_k, F_k, and T_k of the helical polymer: $-(-k\ -\ k+1\ -\ k+2\ -\ k+3)-\ \infty$, where R_k = distance between k and $k+1$, $2F_k$ = angle between $k-1$, k, and $k+1$, and $2T_k$ = torsion angle between $k-1$, k, $k+1$, and $k+2$.

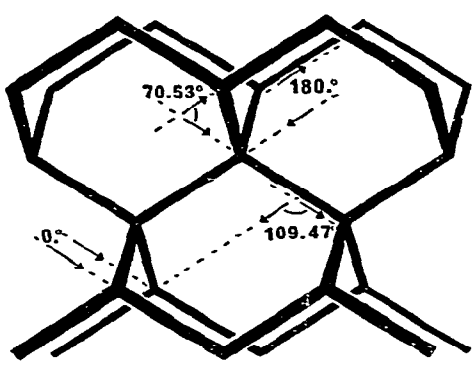

Fig. 2. Diamond-lattice representation of the four possible spatial arrangements of the vectors around which the rotations θ_1 and θ_2 are performed. The corresponding vectorial angle (Γ) can only be given four values: 0°, 180°, Arcos(1/3) $\simeq$ 70.53°, and π − Arcos(1/3) $\simeq$ 109.47°.

TABLE I

COMBINATIONS OF CONFORMATIONS FOR POLYMER CHAINS

θ_1/*Sequence*/θ_2[a]	$\Gamma(°)$[b]	*Subgroup*	*Figure*
None	109.47	IV	[c]
T	180.00	II	4*a*
G^+	70.53	III	5*a*
$T\,T$	109.47	IV	6*a*
$T\,G^+$	109.47	IV	6*b*
$G^+\,G^+$	109.47	IV	6*c*
$G^+\,G^-$	0.0	I	3
$T\,T\,T$	180.00	II	4*b*
$T\,T\,G^+$	70.53	III	5*b*
$T\,G^+\,T$	180.00	II	4*c*
$T\,G^+\,G^+$	70.53	III	5*c*
$T\,G^+\,G^-$	70.53	III	5*d*
$G^+\,T\,G^+$	70.53	III	5*e*
$G^+\,T\,G^-$	180.00	II	4*d*
$G^+\,G^+\,G^+$	180.00	II	4*e*
$G^+\,G^+\,G^-$	70.53	III	5*f*
$G^+\,G^-\,G^+$	70.53	III	5*g*

[a] θ_1 and θ_2 are the two contiguous, variable torsion-angles. The sequences are defined by all the combinations of 1 to 3 torsion angles existing in a *trans* (T), *gauche*$^+$ (G^+) and *gauche*$^-$ (G^-) forms. [b] Γ: see text and Fig. 2 for explanations. [c] The corresponding helical map, being identical to the $\theta_1 TT\theta_2$ one is not given.

perfect tetrahedral value of 109.47°. Thus, each bond within the sequence runs parallel to one of the four tetrahedral directions, as in diamond skeleton. The different combinations of conformations for two successive, variable torsion-angles and for $1 \leqslant (i-2) \leqslant 3$ are given in Table I. An important parameter is the angle Γ between the vectors around which the variable rotations θ_1 and θ_2, in the θ_1/sequence/θ_2 arrangement, are performed. In a diamond lattice, this angle Γ can be assigned only four values: 0, 180, 109.47, and 70.53° (Fig. 2). In each instance, the angle Γ was evaluated and is listed in Table I.

The helical parameters n and h were plotted as *iso-n* and *iso-h* contours on a θ_1–θ_2 surface. It is obvious from the Miyazawa equations[1] that the *iso-n* contours are not dependent of the bond lengths between the i atomic repeat-units. As such, these maps are fairly general. In order to maintain a general presentation, the conformation yielding the maximum extension for a given problem was calculated, and the *iso-h* contours corresponding to 85% of this maximum elongation were plotted*. Furthermore, the contour *iso-h* = 0 was plotted. This contour corresponds to conformations (impossible for infinite chains) in which the path is circular. This contour ($h = 0$) leads to the prediction that cyclic oligomers exhibiting internal C_n symmetry should be capable of existence. Whenever the contours $h = 0$ or $n = 2$ are inter-

*A rule of thumb for the evaluation of energetically allowed regions for polysaccharides sometimes makes use of such a shrinkage of the maximum elongation.

changed, the screw sense of the helix changes to the opposite sense. The chirality of the helix is defined by the sign of n.

RESULTS AND DISCUSSION

Geometrical features of the helical maps. — The maps corresponding to the backbone conformations listed in Table I are given in Figs. 3–6, together with all pertinent information.

Examination of the general features displayed by the *iso-n* contours clearly indicates that four different subgroups are generated (Figs. 3–6). These subgroups are directly related to the spatial arrangement of the vectors around which the θ_1 and θ_2 rotations are performed (see Table I). The first two subgroups are found when the variable rotations are performed around bonds running parallel to each other. In both instances, the *iso-n* contours adopt a linear aspect. When the vectors are *cis*-disposed ($\Gamma = 0°$), the *iso-n* contours are straight lines, parallel to the first bisecting line. This subgroup (I) is found in the set given in Fig. 3. Conversely, when a *trans* arrangement exists ($\Gamma = 180°$), the *iso-n* contours are still straight lines, but they run parallel to the second bisecting line. This subgroup (II) is found in the set given in Fig. 4. The two remaining subgroups are found when the angle between the

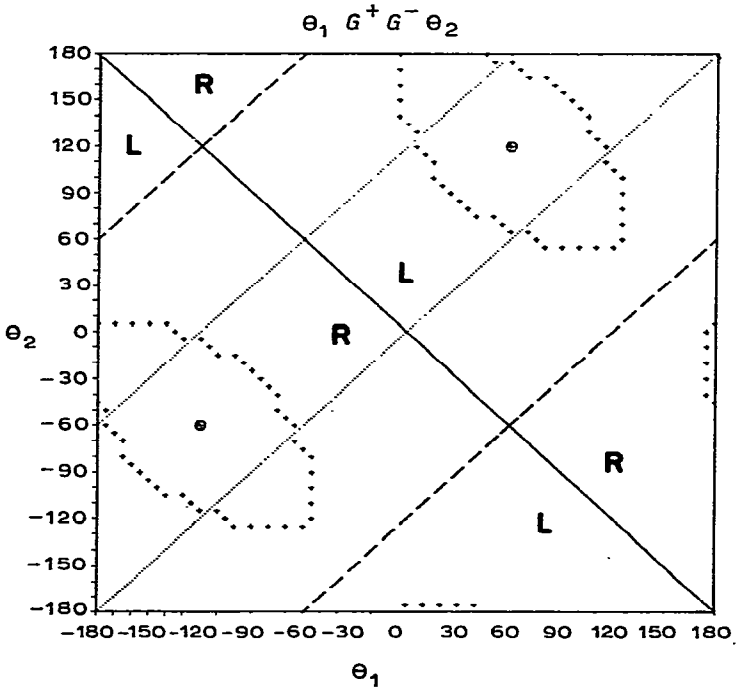

Fig. 3. Helical map of subgroup I, with $\Gamma = 0$. The *iso-n* contours run parallel to the first bisecting line: ——— *iso-h* = 0, — — — — *iso-n* = 2, ... *iso-n* = 3, ... *iso-n* = 4, ... *iso-n* = 5, ⊕ maximal elongation, + + + *iso-h* = 85% of maximal elongation.

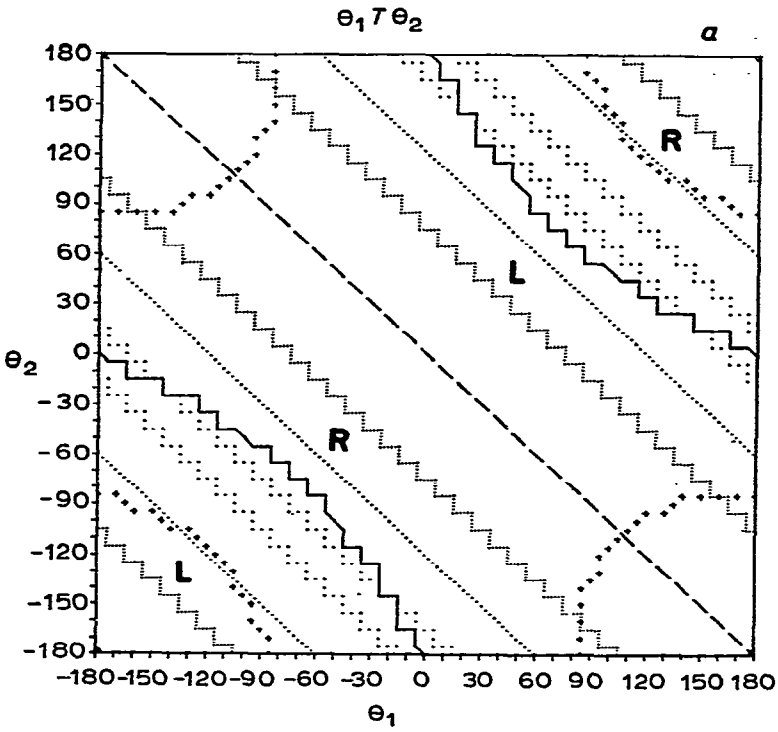
θ1 T θ2
a
180
150
120
90
60
30
0
-30
-60
-90
-120
-150
-180
θ2
R
L
R
L
-180 -150 -120 -90 -60 -30 0 30 60 90 120 150 180
θ1

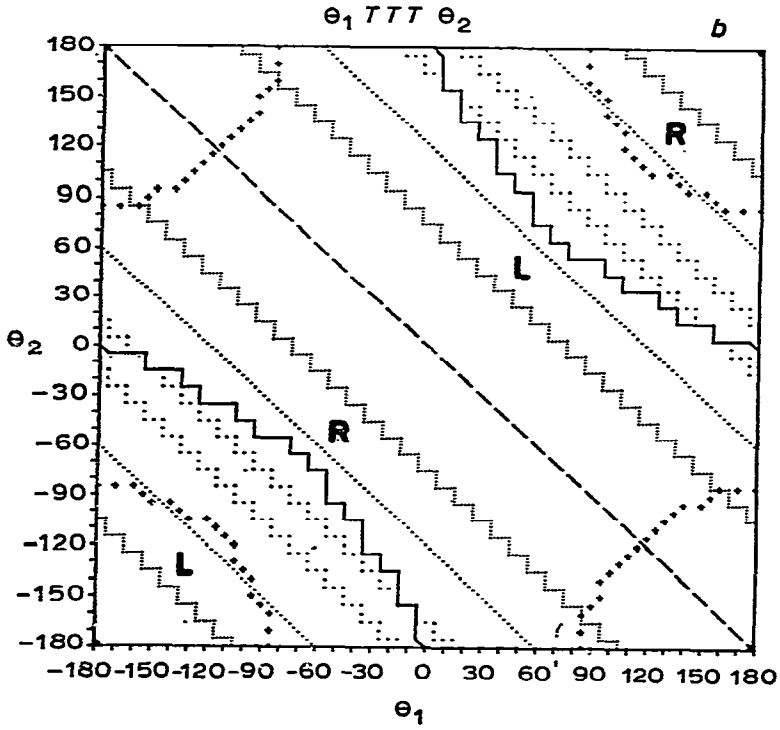
θ1 T T T θ2
b
180
150
120
90
60
30
0
-30
-60
-90
-120
-150
-180
θ2
R
L
R
L
-180 -150 -120 -90 -60 -30 0 30 60 90 120 150 180
θ1

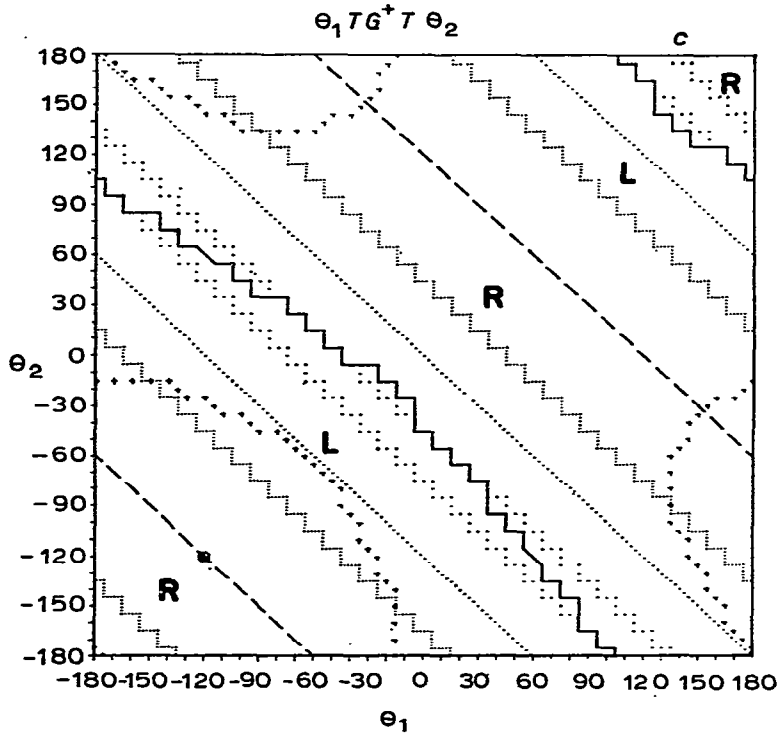
θ1TG+Tθ2
c
R
L
R
L
R
θ2
θ1
180
150
120
90
60
30
0
-30
-60
-90
-120
-150
-180
-180 -150 -120 -90 -60 -30 0 30 60 90 120 150 180

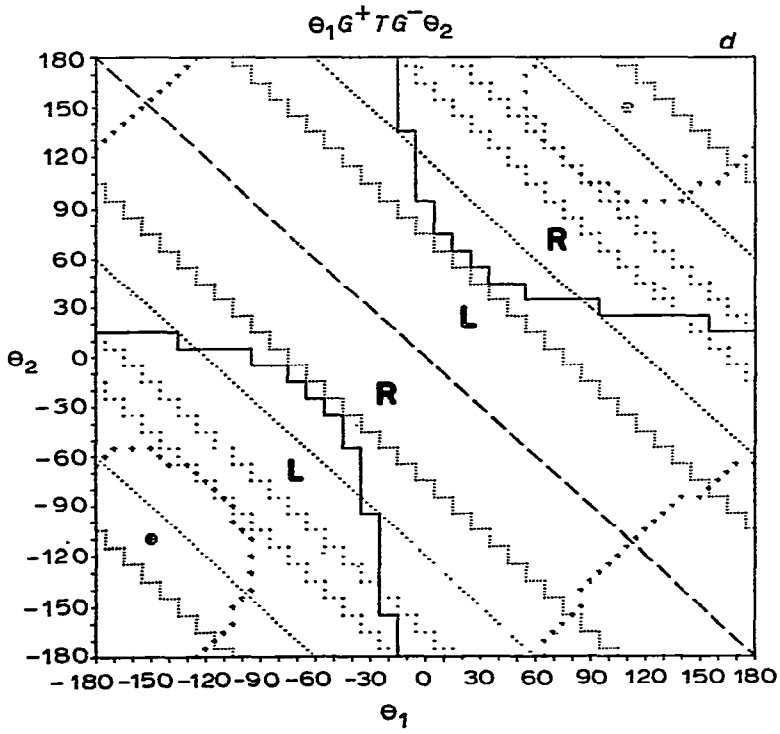
θ1G+TG−θ2
d
R
L
R
L
θ2
θ1
180
150
120
90
60
30
0
-30
-60
-90
-120
-150
-180
-180 -150 -120 -90 -60 -30 0 30 60 90 120 150 180

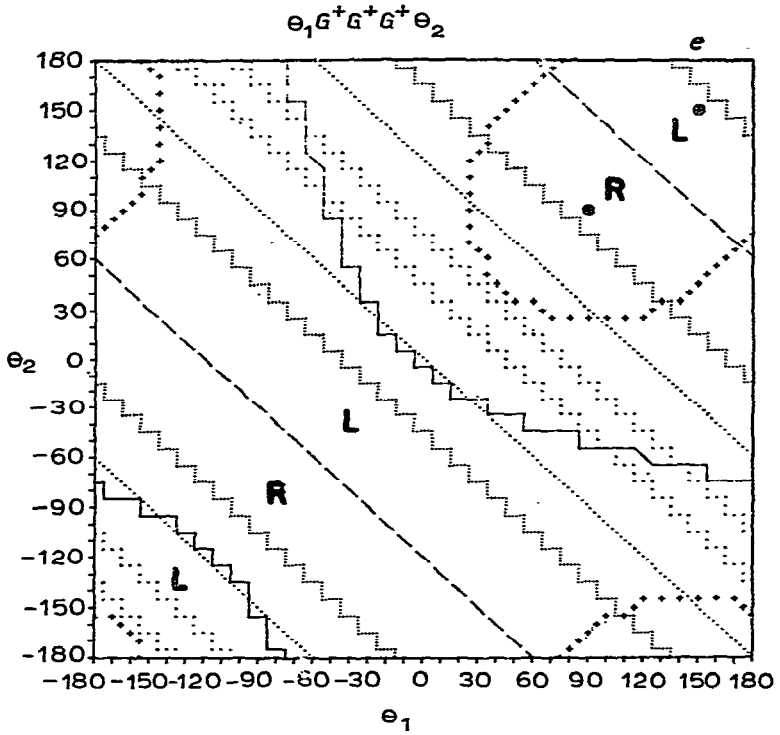

Fig. 4. Helical maps of subgroup II, with $\Gamma = 180$. The *iso-n* contours run parallel to the second bisecting line: symbols are as in Fig. 3.

vectors, around which the variable rotations are performed, corresponds to the tetrahedral angle and its supplement. When the angle between θ_1 and θ_2 is $\Gamma = 70.53°$, a "circle-like picture" is obtained for all of the *iso-n* contours except $n = 2$. In this instance, the set of *iso*-2 is "degenerate", as two perpendicular lines are obtained. This subgroup (III) is found in the set given in Fig. 5. The fourth subgroup is obtained for a value of the vectorial angle equal to the tetrahedral angle: $\Gamma = 109.47°$. Here, an "elliptical-like picture" is obtained, as may be seen in Fig. 6. There thus exists a direct relation between the spatial arrangement of the vectors around which the variable rotations are performed and the corresponding *iso-n* contours. Although this classification is satisfying in itself, it may be expressed in terms of mathematical expressions. From the Miyazawa equations[1], a mathematical expression for the *iso-n* contours may be derived as:

$$\alpha_1 \cos(S) + \alpha_2 \cos(D) = 1,$$

where

$$S = \frac{\theta_1 + \theta_2}{2} + \Delta_s \qquad \text{and} \qquad D = \frac{\theta_1 - \theta_2}{2} + \Delta_d,$$

α_1 and α_2 are coefficients expressing the non-variable moiety of the helix, and Δ_s

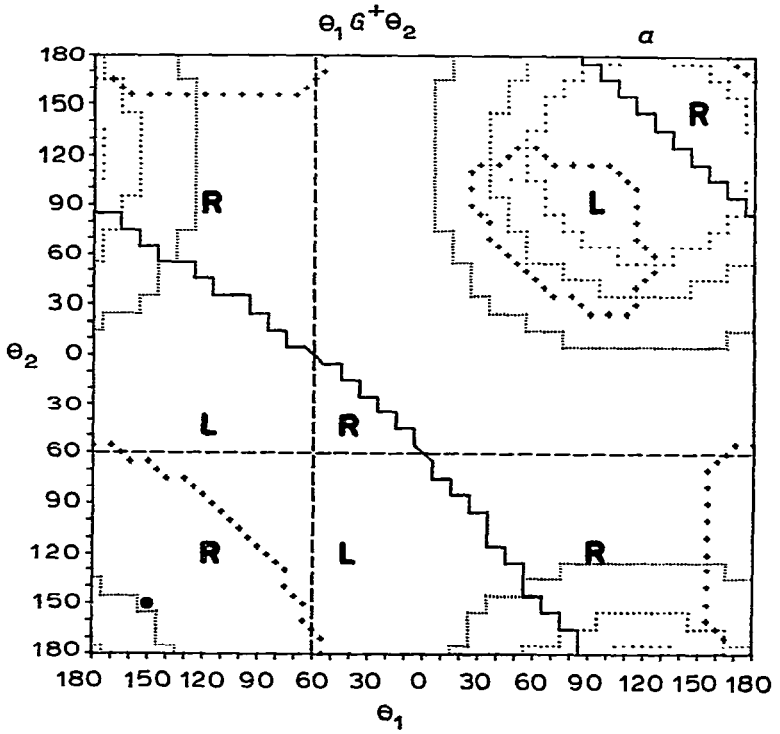
θ1 G+ θ2
a
R
L
R
L
R
L
R
180 150 120 90 60 30 0 30 60 90 120 150 180
θ2
θ1

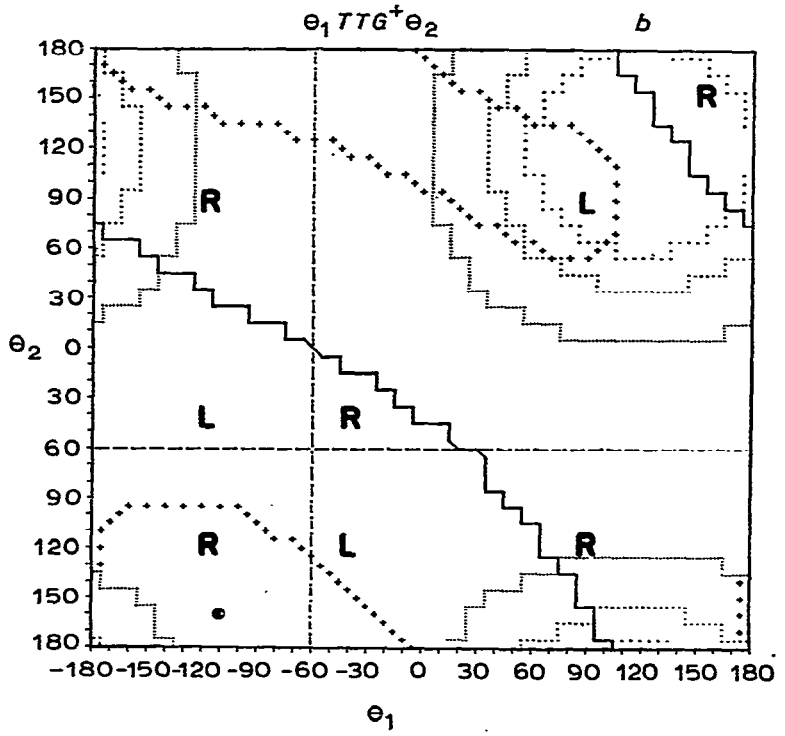
θ1 TTG+ θ2
b
R
L
R
L
R
L
R
-180 -150 -120 -90 -60 -30 0 30 60 90 120 150 180
θ2
θ1

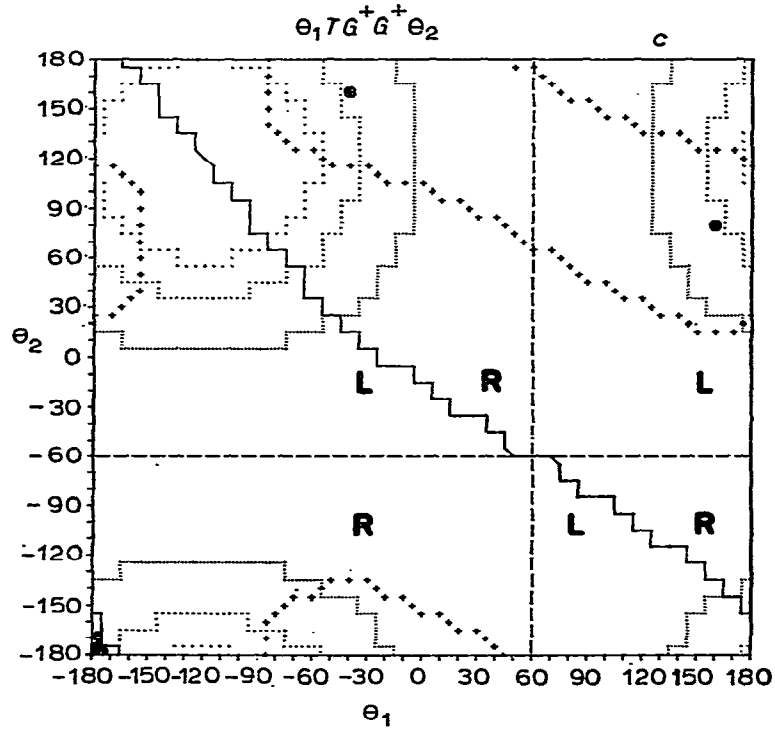
θ1TG+G+θ2
c
180
150
120
90
60
30
θ2 0
-30
-60
-90
-120
-150
-180
L
R
L
R
L
R
-180 -150 -120 -90 -60 -30 0 30 60 90 120 150 180
θ1

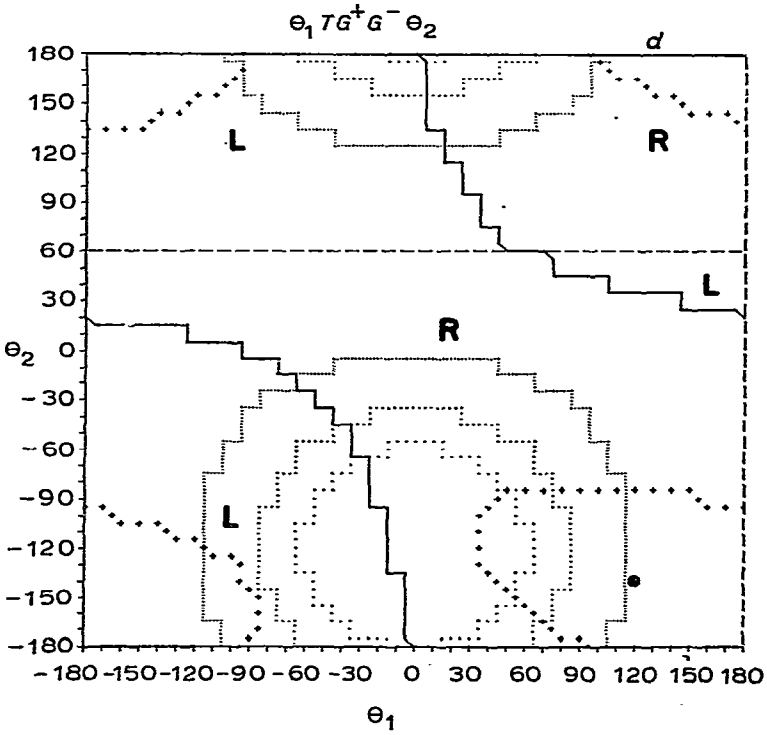
θ1TG+G−θ2
d
180
150
120
90
60
30
θ2 0
-30
-60
-90
-120
-150
-180
L
R
L
R
L
-180 -150 -120 -90 -60 -30 0 30 60 90 120 150 180
θ1

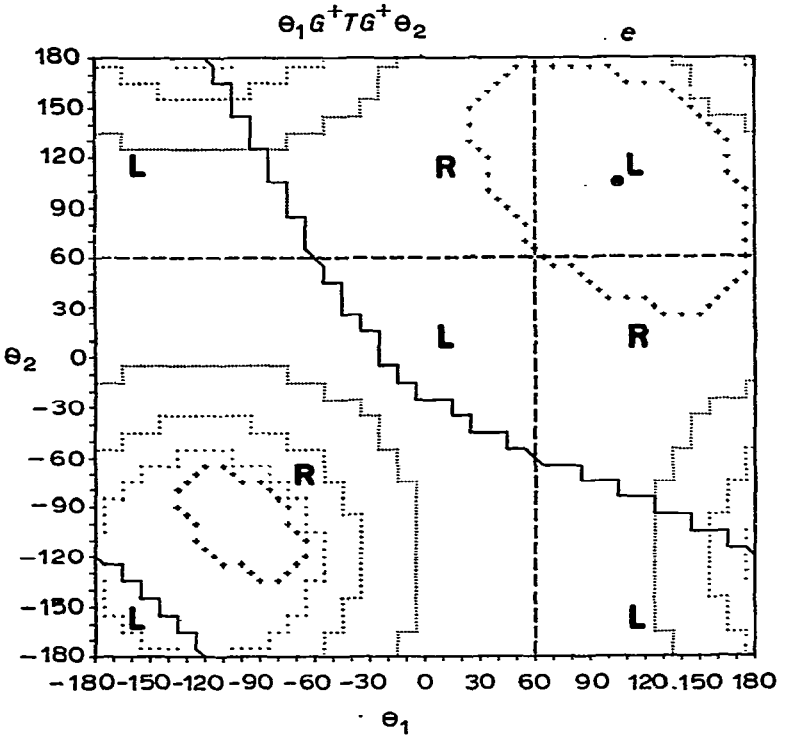
$\theta_1 G^+ T G^+ \theta_2$
e
180
150
120
90
60
30
0
-30
-60
-90
-120
-150
-180
θ_2
L
R
L
L
R
R
L
L
-180 -150 -120 -90 -60 -30 0 30 60 90 120 150 180
θ_1

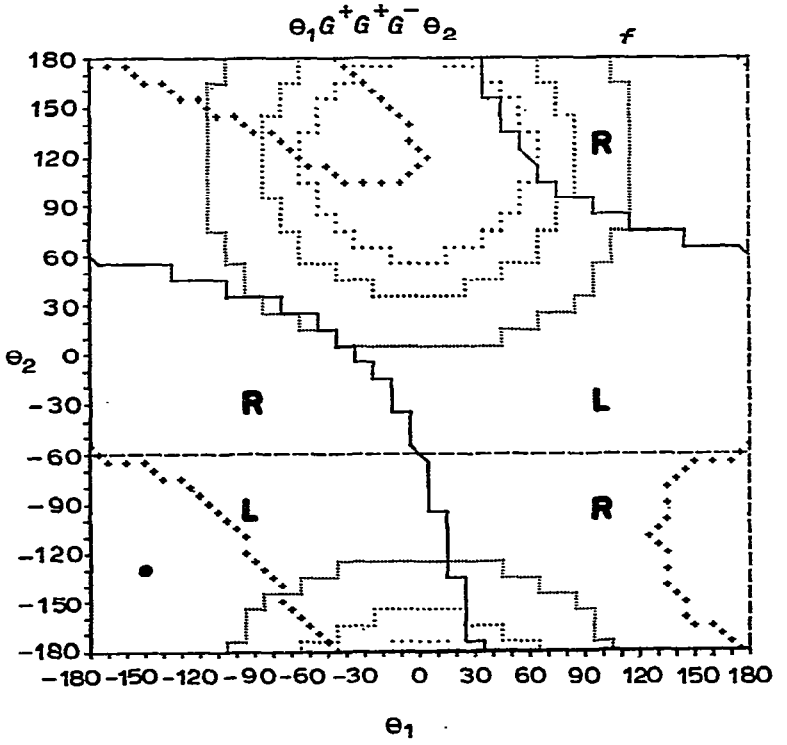
$\theta_1 G^+ G^+ G^- \theta_2$
f
180
150
120
90
60
30
0
-30
-60
-90
-120
-150
-180
θ_2
R
R
L
L
R
-180 -150 -120 -90 -60 -30 0 30 60 90 120 150 180
θ_1

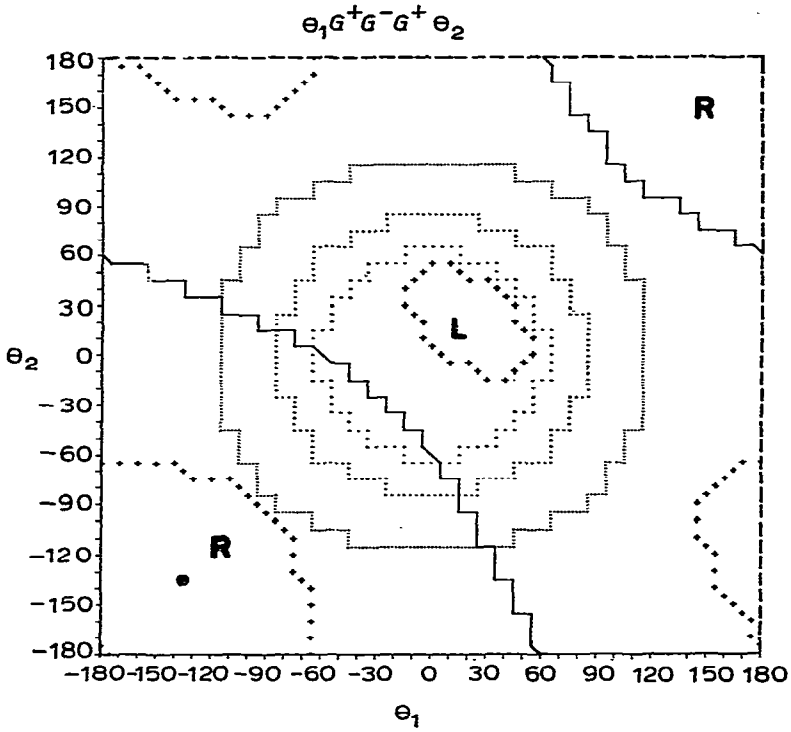

Fig. 5. Helical maps of subgroup III, with $\Gamma = 70.53$. The *iso-n* contours exhibit a "circle-like picture": symbols are as in Fig. 3.

and Δ_d are translational terms arising from the centering of the curves at θ_1 and θ_2 equal to zero. According to the respective values of α_1 and α_2, the four different subgroups just mentioned generate the following:

$\alpha_1 \neq 0 \quad \alpha_2 = 0$: subgroup (I),
$\alpha_1 = 0 \quad \alpha_2 \neq 0$: subgroup (II),
$\alpha_1 = \alpha_2 \quad (\alpha_1 \neq 0, \alpha_2 \neq 0)$: subgroup (III),
and $\alpha_1 \neq \alpha_2 \quad (\alpha_1 \neq 0, \alpha_2 \neq 0)$: subgroup (IV),

Therefore, it may be stated that, in the case of two contiguous torsion-angles, and with the use of a diamond-lattice representation, *only* four different types of *iso-n* curves can be generated.

Because of the strong dependence of *iso-h* contours on such internal parameters as bond lengths and bond angles, any type of extrapolation is somewhat hampered. As such, each combination of conformations listed in Table I, gives rise to a specific set of *iso-h* contours. One example of such a specificity is given in Fig. 7. In this Figure, the *iso-h* contour corresponding to 15% of the maximum elongation of the θ_1 $G^+G^+G^+$ θ_2 sequence is drawn, together with the *iso-n* contours. Examination of the number of intersections of *iso-h* and *iso-n* contours shows that, for *iso-n* $= \pm 5$

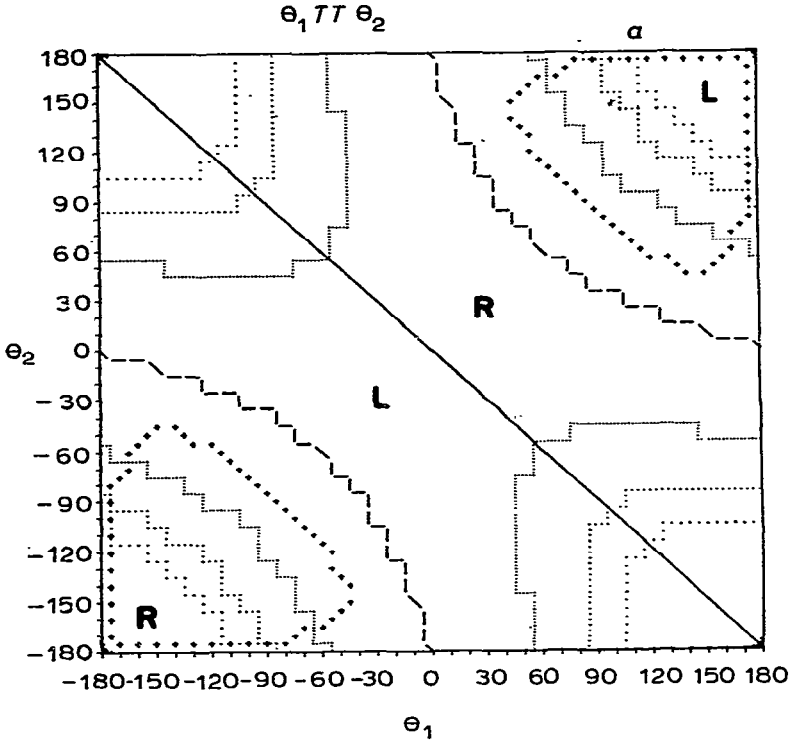
θ1 TT θ2
a
L
R
L
R
θ2
θ1
180
150
120
90
60
30
0
-30
-60
-90
-120
-150
-180
-180 -150 -120 -90 -60 -30 0 30 60 90 120 150 180

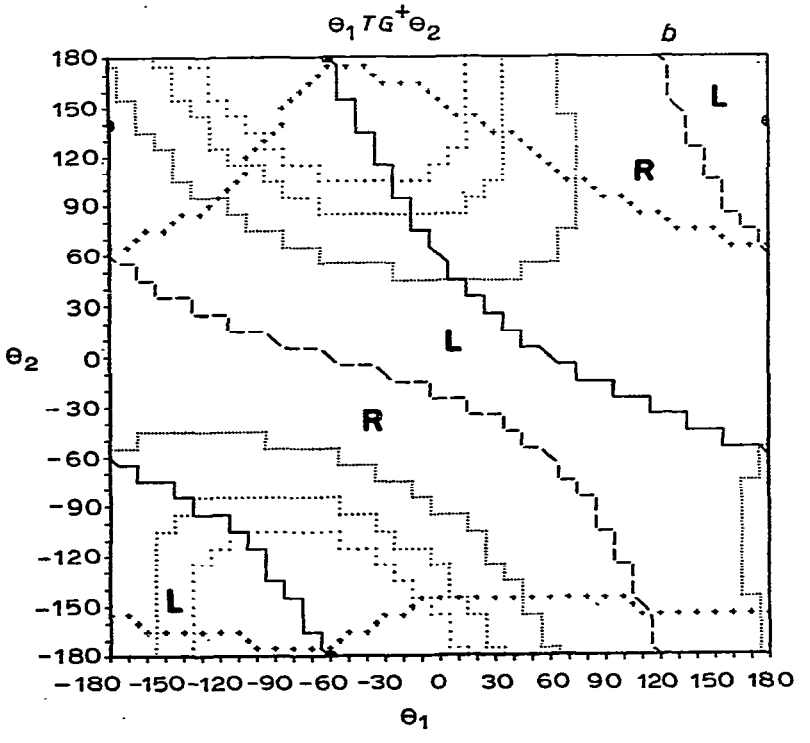
θ1 TG+ θ2
b
L
R
L
R
L
θ2
θ1
180
150
120
90
60
30
0
-30
-60
-90
-120
-150
-180
-180 -150 -120 -90 -60 -30 0 30 60 90 120 150 180

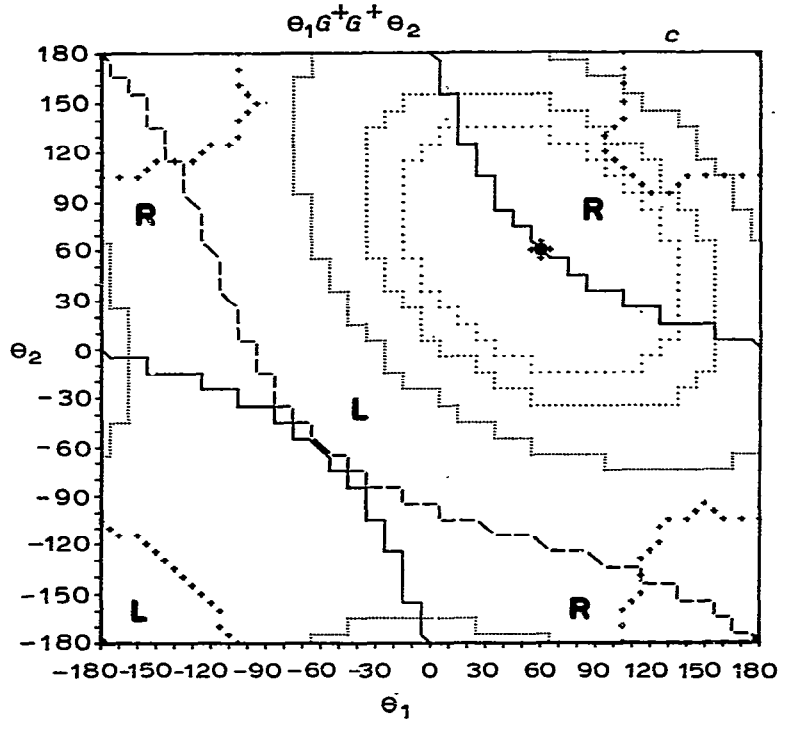

Fig. 6. Helical maps of subgroup IV, with $\Gamma = 109.47$. The *iso-n* contours exhibit an "elliptical-like picture": symbols are as in Fig. 3.

and *iso-h* = 15%, eight points (expressed in terms of θ_1 and θ_2) are found. Thus the number of conformations (θ_1, θ_2) can amount to eight for an unspecified chirality. This finding has been further corroborated by explicitely solving the set of mathematical equations giving all of the θ_1 and θ_2 values, n and h being specified[12].

Applications to homopolysaccharides and cyclic oligosaccharides. — The series of calculated *n,h* maps is well suited for use with a broad range of polymers. For example, the $\theta_1 T \theta_2$ map covers the whole series of secondary structures predictable for polypeptides. It is beyond the scope of this paper to give many other examples. However, with regard to homopolysaccharides, it may be recognized that some of the helical maps readily accommodate some previous studies. For example, the $\theta_1 TG^+G^+\theta_2$ map (Fig. 5*c*) and the $\theta_1 TG^+T\theta_2$ map (Fig. 4*c*) are reminiscent of the helical maps obtained for amylose[13] and for cellulose[14], respectively. This finding is of interest because it illustrates that, at least in the first step of a structural investigation, the glucopyranose residue may be expressed by using a geometry derived from the diamond-lattice representation. The correlation between the maps obtained and all realizable types of helical structure in those homopolysaccharides made up of hexopyranoside units is given in Table II. The data in Table II were generated by considering the combinations arising from the absolute configuration *R* and *S* at atoms

TABLE II

CORRELATIONS BETWEEN THE HELICAL MAPS AND ALL GEOMETRICALLY REALIZABLE TYPES OF HELICAL STRUCTURES WITHIN THE HOMOPOLYSACCHARIDE SERIES, MADE UP OF HEXOPYRANOSIDES UNITS POLYMERIZED THROUGH (1→2), (1→3), AND (1→4) LINKAGES

Configuration[b] *at*			*Linkage type*	*Anomeric configuration*	*Ring conformation*	*Glycosidic junction*[a] A_{C-2}-(1→2)-A_{C-2}			*Glycosidic junction*[a] A_{C-3}-(1→3)-A_{C-3}			*Glycosidic junction*[a] A_{C-4}-(1→4)-A_{C-4}		
C-1	*C-5*	*C-1*				$A_{C-2} = A_R$ *allose galactose glucose gulose* Φ_H	*i*=2 *Helical maps*[d]	$A_{C-2} = A_S$ *altrose idose mannose talose* Ψ_H	$A_{C-3} = A_R$ *allose altrose gulose idose* Φ_H	*i*=3 *Helical maps*[d]	$A_{C-3} = A_S$ *galactose glucose mannose talose* Ψ_H	$A_{C-4} = A_R$ *galactose gulose idose talose* Φ_H	*i*=4 *Helical maps*[d]	$A_{C-4} = A_S$ *allose altrose glucose mannose* Ψ_H
R	*R*	*R*	*a*	β-D	$^1C_4$	θ_1 −120	*T*	θ_2 −120	θ_2 −120	TG^+	θ_1 −120	$-\theta_2$ +120	TG^+G^{+*}	$-\theta_1$ −120
R	*R*	*R*	*e*	β-D	$^4C_1$	$-\theta_1$ −120	G^{+*}	$-\theta_2$ −120	θ_1 −120	TG^+	θ_2 −120	θ_1 +120	TG^+G^+	θ_2 −120
R	*R*	*S*	*a*	α-D	$^4C_1$	θ_1 +120	G^+	θ_2 −120	θ_2 +120	G^+G^-	θ_1 −120	θ_1 −120	$G^+G^+G^+$	θ_2 −120
R	*R*	*S*	*e*	α-D	$^1C_4$	$-\theta_1$ +120	G^{+*}	$-\theta_2$ −120	θ_1 +120	*TT*	θ_2 −120	$-\theta_1$ −120	TG^+T^*	$-\theta_2$ −120
R	*S*	*R*	*a*	α-L	$^1C_4$	$-\theta_1$ −120	G^{+*}	$-\theta_2$ +120	θ_1 −120	G^+G^-	θ_2 +120	$-\theta_1$ +120	$G^+G^+G^{+*}$	$-\theta_2$ +120
R	*S*	*R*	*e*	α-L	$^4C_1$	θ_1 −120	G^+	θ_2 +120	θ_1 −120	*TT*	θ_2 +120	$-\theta_1$ +120	TG^+T^*	$-\theta_2$ +120
R	*S*	*S*	*a*	β-L	$^4C_1$	θ_1 +120	*T*	θ_2 +120	θ_2 +120	TG^+	θ_1 +120	θ_2 −120	TG^+G^+	θ_1 +120
R	*S*	*S*	*e*	β-L	$^1C_4$	θ_1 +120	G^+	θ_2 +120	$-\theta_1$ +120	TG^{+*}	$-\theta_2$ +120	$-\theta_1$ −120	TG^+G^{+*}	$-\theta_2$ +120
S	*R*	*R*	*a*	β-D	$^1C_4$	$-\theta_1$ −120	G^{+*}	$-\theta_2$ +120	θ_1 −120	G^+G^-	θ_2 +120	$-\theta_1$ +120	$G^+G^+G^{+*}$	$-\theta_2$ +120
S	*R*	*R*	*e*	β-D	$^4C_1$	θ_1 −120	G^+	θ_2 +120	θ_1 −120	*TT*	θ_2 +120	θ_1 +120	TG^+T	θ_2 +120
S	*R*	*S*	*a*	α-D	$^4C_1$	θ_1 +120	*T*	θ_2 +120	θ_2 +120	TG^+	θ_1 +120	θ_2 −120	TG^+G^+	θ_1 +120
S	*R*	*S*	*e*	α-D	$^1C_4$	θ_1 +120	G^+	θ_2 +120	$-\theta_1$ +120	TG^{+*}	$-\theta_2$ +120	$-\theta_1$ −120	TG^+G^{+*}	$-\theta_2$ +120
S	*S*	*R*	*a*	α-L	$^1C_4$	θ_1 −120	*T*	θ_2 −120	θ_2 −120	TG^+	θ_1 −120	$-\theta_2$ +120	TG^+G^{+*}	$-\theta_1$ −120
S	*S*	*R*	*e*	α-L	$^4C_1$	$-\theta_1$ −120	G^{+*}	$-\theta_2$ −120	θ_1 −120	TG^+	θ_2 −120	θ_1 +120	TG^+G^+	θ_2 −120
S	*S*	*S*	*a*	β-L	$^4C_1$	θ_1 +120	G^+	θ_2 −120	θ_2 +120	G^+G^-	θ_1 −120	θ_1 −120	$G^+G^+G^+$	θ_2 −120
S	*S*	*S*	*e*	β-L	$^1C_4$	$-\theta_1$ +120	G^{+*}	$-\theta_2$ −120	θ_1 +120	*TT*	θ_2 −120	$-\theta_1$ −120	TG^+T^*	$-\theta_2$ −120

[a]For a given (1→*i*) glycosidic linkage (having *i* = 2, 3, or 4), the common name of the hexopyranoside unit, which depends on the *R* or *S* configuration at C-*i*, is given as A_{C-i}. [b]The configurations at atoms C-*i*, C-5, and C-1 are either *R* or *S*. The linkage type is either axial (*a*) or equatorial (*e*). Very simple rules may be delineated: (a) the *R* configuration at C-5 implies D and conversely *S* implies L; (b) The anomeric configuration (α or β) arises from the "product" of the configurations at C-1 and C-5, namely, $C\text{-}1_R \times C\text{-}5_R \rightarrow \beta$; $C\text{-}1_R \times C\text{-}5_S \rightarrow \alpha$; $C\text{-}1_S \times C\text{-}5_S \rightarrow \beta$; $C\text{-}1_S \times C\text{-}5_R \rightarrow \alpha$; (c) Similarly, the chair conformation may be readily deduced from the "product" of the configuration at C-1 by the linkage type at C-1: $C\text{-}1_R \times a \rightarrow {}^1C_4$; $C\text{-}1_R \times e \rightarrow {}^4C_1$; $C\text{-}1_S \times e \rightarrow {}^1C_4$; $C\text{-}1_S \times e \rightarrow {}^4C_1$. [c]For the (1→4) linkage, there exists two possible ways to build up a fixed sequence of atoms. In this situation, we have always considered the sequence incorporating O-5. [d]The relevant helical maps to be used are given in adherence to the sequences listed in Table I. When such a sequence is followed by (*), the chirality indicated on the corresponding map must be reversed. Because the Cahn–Ingold–Prelog rule cannot be used when the substitution mode of atom C-*i* is unknown, the glycosidic torsion-angles have been systematically referred to the hydrogen atoms. As such, the glycosidic torsion-angles between two contiguous *j* and *j*+1 residues, (1→3)-linked are: $\Phi_H = H_j\text{-}1\text{-}C_j\text{-}1\text{-}O_j\text{-}1\text{-}C_{j+1}\text{-}3$, and $\Psi_H = C_j\text{-}1\text{-}O_j\text{-}1\text{-}C_{j+1}\text{-}3\text{-}H_{j+1}\text{-}3$.

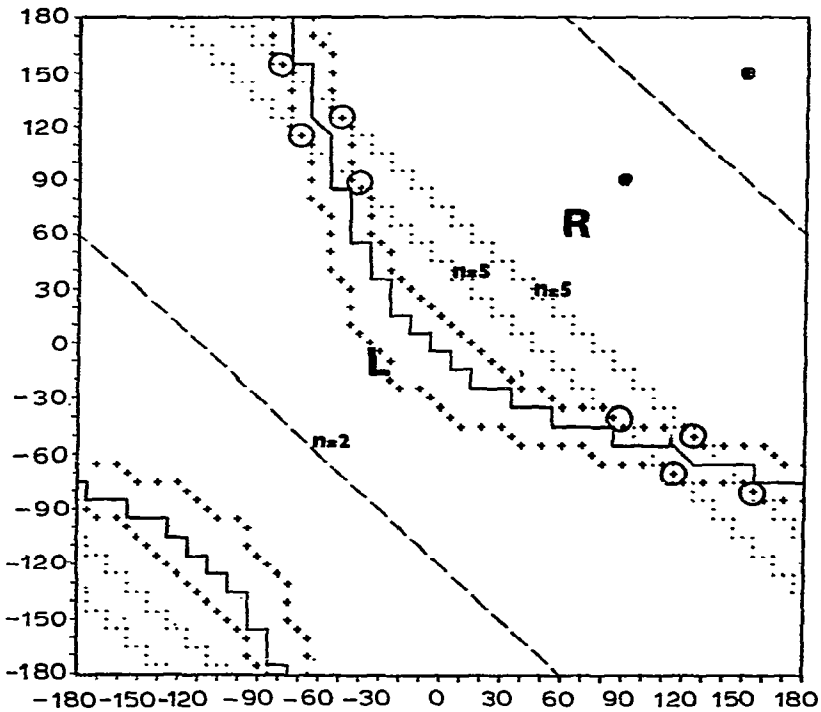

Fig. 7. Helical map of the θ_1 $G^+G^+G^+$ θ_2 sequence. The *iso-h* (+ + +) contour corresponds to 15% of the maximal elongation ⊕. The eight possible intersections of this contour having *iso-n* = ±5 are shown as 0; ——— *iso-h* = 0, — — — — *iso-n* = 2, ... *iso-n* = 5, ⊕ Maximum elongation, ÷ + + *iso-h* = 15% of maximum elongation.

TABLE III

SOME EXAMPLES OF THE APPLICATION OF TABLE II (1→2)-, (1→3)-, AND (1→4)-LINKED TO HOMOPOLYSACCHARIDES

Homopolysaccharide		*Configuration at*			*Linkage type*
		C-i	*C-5*	*C-1*	
(1→2)-α-D-Glucan	($^4C_1$)	*R*	*R*	*S*	a
(1→3)-α-D-Glucan	($^4C_1$)	*S*	*R*	*S*	a
(1→4)-α-D-Glucan	($^4C_1$)	*S*	*R*	*S*	a
(1→2)-β-D-Glucan	($^4C_1$)	*R*	*R*	*R*	e
(1→3)-β-D-Glucan	($^4C_1$)	*S*	*R*	*R*	e
(1→4)-β-D-Glucan	($^4C_1$)	*S*	*R*	*R*	e
(1→4)-β-D-Galactan	($^4C_1$)	*R*	*R*	*R*	e
(1→4)-α-L-Fucan	($^1C_4$)	*R*	*S*	*R*	a

C-1, C-5, and C-i [where i = 2, 3, and 4, is associated with a given (1→i) glycosidic linkage] and the axial or equatorial disposition at C-1. It is shown that a total of eight helical maps cover all instances generated. Thus, all eight hexopyranoside monosaccharides, either D or L, occurring in the $^4C_1$ or $^1C_4$ conformation, and polymerizing through (1→2), (1→3), or (1→4) linkages, either α or β, are accommodated. Table III lists some examples of homopolysaccharides, together with the relevant information leading to the helical maps useful in their structural investigation.

A further situation involves (1→6)-linked chains. Such a glycosidic linkage between residues j and $j + 1$, offers three contiguous variable torsion angles Φ, Ψ, and Ω, where:

$$\Phi = (O_j\text{-}5 - C_j\text{-}1 - O_j\text{-}1 - C_{j+1}\text{-}6)$$
$$\Psi = (C_j\text{-}1 - O_j\text{-}1 - C_{j+1}\text{-}6 - C_{j+1}\text{-}5)$$
$$\Omega = (O_j\text{-}1 - C_{j+1}\text{-}6 - C_{j+1}\text{-}5 - O_{j+1}\text{-}5)$$

However, recent results derived from a statistical survey of crystal structures of mono and oligosaccharides[15], as well as energy calculations[9], have shown that only three stable dispositions exist about the angle Ω. Furthermore, only slight variations away from these non-eclipsing dispositions are observed[15]. This result indicates that the helical conformations of any homopolysaccharide (1→6) links may be studied by successively assigning to the angle Ω a fixed value corresponding to a stable conformation, and then using the relevant two-dimensional, helical map. The pertinent maps to be used for investigation of secondary structures of α-(1→6)- and β-(1→6)-linked homopolysaccharides are given in Table IV.

Apart from cyclic molecules made up of (1→4)-α-D-glucopyranosyl residues, cyclic oligosaccharides do not occur widely. However, the use of cyclic oligosaccharides as model compounds is of interest; such systems offer a perfect simulation of the related polysaccharides as end-effects are eliminated *de facto*. In the course of chemical synthesis of a (1→6)-β-D-glucan, a cyclic tetramer, namely [*O*-β-D-glucopyranosyl-(1→6)$_4$ 1,6″′ anhydride dodecaacetate was formed[16]. ^{13}C-N.m.r. spectroscopy indicates a chair conformation for the rings and internal C_4 symmetry (within the n.m.r. time-scale) for the tetrasaccharide. Furthermore, preliminary studies indicate that single crystals may be grown from solution. The conformational investigation of such a cyclic system can be performed either by using the relevant helical maps, or by calculating all possible combinations of Φ, Ψ, and Ω giving rise to a cyclic tetrasaccharide, and then computing the energy associated with all of the resulting conformations. Fig. 8 is a schematic diagram of such a cyclic tetramer, incorporating the relevant torsion angles. By using a diamond-lattice representation for the glucosyl residue, χ_1 and χ_2 must be maintained in a *trans*-disposition, corresponding to the $^4C_1$ chair form. Only three parameters remain to be determined. The first approach makes use of the existence of the three stable, non-eclipsing dispositions around the angle Ω. Hence, only three helical maps have to be examined. With the aid of Table V and Figs. 4*b* and 5*b*, the values of Φ, Ψ, and Ω corresponding to the occurrence of a cyclic tetramer having a β-(1→6) linkage, may readily be deter-

TABLE IV

CORRELATION BETWEEN THE HELICAL MAPS AND ALL GEOMETRICALLY REALIZABLE TYPES OF HELICAL STRUCTURES OF (1→6)-LINKED HEXOPYRANOSYL HOMOPOLYSACCHARIDES

Configuration at		*Linkage type*	*Anomeric disposition*	*Ring conformation*	Φ	*Helical maps*	Ψ	Ω
C-5	*C-1*							
					θ_2	TG^+G^-	θ_1	180
R	*R*	*a*	β-D	$^1C_4$	θ_2	$G^+G^+G^-$	θ_1	+60
					$-\theta_1$	$G^+G^-G^{+*}$	$-\theta_2$	−60
					θ_1	TTT	θ_2	180
R	*R*	*e*	β-D	$^4C_1$	θ_1	TTG^+	θ_2	+60
					$-\theta_1$	TTG^{+*}	$-\theta_2$	−60
					θ_2	TTG^+	θ_1	180
R	*S*	*a*	α-D	$^4C_1$	θ_1	G^+TG^+	θ_2	+60
					θ_1	G^+TG^-	θ_2	−60
					θ_1	TG^+T	θ_2	180
R	*S*	*e*	α-D	$^1C_4$	θ_1	TG^+G^+	θ_2	+60
					θ_1	TG^+G^-	θ_2	−60
					$-\theta_2$	TTG^{+*}	$-\theta_1$	180
S	*R*	*a*	α-L	$^1C_4$	θ_2	G^+TG^-	θ_1	+60
					$-\theta_1$	G^+TG^{+*}	$-\theta_2$	−60
					$-\theta_1$	TG^+T^*	$-\theta_2$	180
S	*R*	*e*	α-L	$^4C_1$	$-\theta_1$	TG^+G^{-*}	$-\theta_2$	+60
					$-\theta_1$	TG^+G^{-*}	$-\theta_2$	−60
					$-\theta_2$	TG^+G^{-*}	$-\theta_1$	180
S	*S*	*a*	β-L	$^4C_1$	θ_1	$G^+G^-G^-$	θ_2	+60
					$-\theta_2$	$G^+G^+G^{-*}$	$-\theta_1$	−60
					θ_1	TTT	θ_2	180
S	*S*	*e*	β-L	$^1C_4$	θ_1	TTG^+	θ_2	+60
					$-\theta_1$	TTG^{+*}	$-\theta_2$	−60

mined. As the value of 180° for the angle Ω cannot yield the tetrasaccharide investigated (helical map $\theta_1 TTT\theta_2$, Fig. 4*b*), only four sets of Φ, Ψ, and Ω angles are found:

$$\Phi = 95°,\ \Psi = -160°,\ \Omega = 60°,$$
$$\Phi = -175°,\ \Psi = 70°,\ \Omega = 60°,$$
$$\Phi = -95°,\ \Psi = 160°,\ \Omega = -60°,$$
and $$\Phi = 175°,\ \Psi = -70°,\ \Omega = -60°,$$

In order to further corroborate the present finding, a complete analysis was undertaken, first by analyzing the combinations of Φ, Ψ, and Ω giving rise to a cyclic tetramer. The energy associated with all relevant conformations was then calculated. The glucose residues approximated the diamond lattice, all bond lengths being 1.54 Å. The hydrogen positions used were computed according to a perfect tetrahedral arrangement; a value of 1.09 Å being assigned to C–H distances. The first step was performed by generating four contiguous glucose residues having the same torsion-angle values

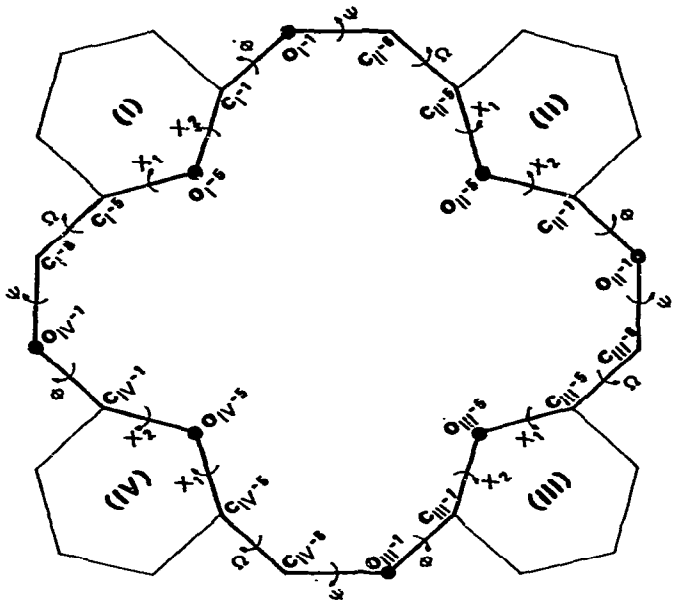

Fig. 8. Schematic diagram of a cyclic tetrasaccharide made up of (1→6)-β-D-glucopyranosyl residues. A diamond-lattice representation is used. All C–C bond-lengths are given the value 1.54 Å, and the bond angles are assigned a perfect tetrahedral value of 109.47°. χ_1, χ_2, Φ, Ψ, and Ω are the torsion angles along the backbone.

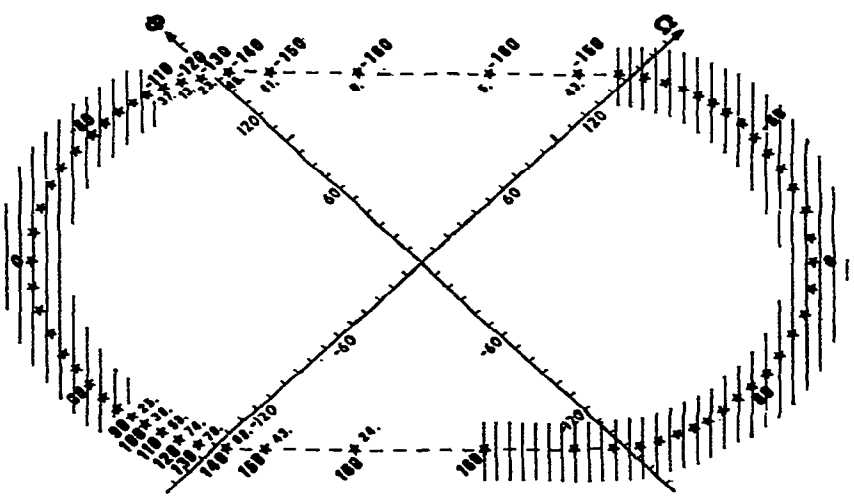

Fig. 9. Diagram of the (Φ, Ψ, Ω) combinations giving rise to a cyclic, β-D-(1→6)-linked tetrasaccharide. The values of Ψ are indicated on the contour, together with the energy (kcal.mol^{-1}) associated with the relevant combinations.

TABLE V

SOME EXAMPLES OF THE APPLICATION OF TABLE IV TO (1→6)-LINKED HOMOPOLYSACCHARIDES

Homopolysaccharide	*Configuration at*		*Linkage type*
	C-5	*C-1*	
(1→6)-α-D-Glucan ($^4C_1$)	*R*	*S*	*a*
(1→6)-β-D-Glucan ($^4C_1$)	*R*	*R*	*e*

at the glycosidic linkage. At this stage, the cyclic stress was introduced, that is, the distance between the first and the (N + 1) atom was made equal to zero. This was achieved by minimizing the distance by use of a Simplex procedure[17]. These calculations were made at 10° intervals in the value of Ψ over the range $-180 < \Psi < 180°$. At this stage, it was noted that a given value of Ψ, within the −160°, +160° interval, generated[18] two pairs of torsion angles (Φ,Ω). The resulting curve is depicted in Fig. 9. The energy associated with each combination of Φ, Ψ, and Ω belonging to this curve was computed and appropriately recorded in Fig. 9. The energy was evaluated by using the following function[19]:

$$E = \sum_{i>m} 2.25\,\varepsilon_{im}\left(\frac{d_{im}}{r_{im}}\right)^6 + 8.28\,10^5\,e^{-(r_{im}/0.0736\,d_{im})},$$

where r_{im} is the distance between two non-bonded atoms, d_{im} is the sum of van der Waals radii for a given pair of non-bonded atoms, and $\varepsilon_{im} = (\varepsilon_i + \varepsilon_m)^{1/2}$ was evaluated by using the following constants $\varepsilon_C = 0.04$, $\varepsilon_O = 0.07$, and $\varepsilon_H = 0.10$. The calculations indicate that only two segments are energetically favored, and that a value of Ω equal to 180° cannot yield the cyclic tetrasaccharide. Within a given segment, two energy minima are found. It is noteworthy that two, among the four combinations of Φ, Ψ, and Ω as determined from the helical maps, belong to these segments. Indeed, one of them ($\Phi = 95°$, $\Psi = -160°$, and $\Omega = 60°$) corresponds to the deepest energy minimum. The other one, ($\Phi = -95°$, $\Psi = 160°$, and $\Omega = -60°$) belongs to the other segment. Hence, the predictions deduced from the very simple approach making use of helical maps are corroborated. Because of the approximations occurring from the use of a diamond-lattice idealization of the glucose residues, differences of the order of 30 kcal.mol^{-1} might not be significant, and conformations belonging to the two segments might be expected to occur. However, it should be noted that one of these segments involves values of Φ near 100°. Such a value is quite opposite to the value of approximately −80° for Φ usually found in the crystal structures of glycosides and oligosaccharides containing the β-D linkage[20].

CONCLUSION

The results reported here provide direct information on helical maps for given monomeric sequences as a function of two, variable torsion-angles. Within the

limited range of combinations of structural backbones studied in this work, the maps obtained are readily applicable to several classes of polymer, such as polypeptides and homopolysaccharides. Furthermore, straightforward prediction of the existence of cyclic oligomers is feasible. Geometrical criteria underlying the general features of the helical maps have been elucidated. There exists a direct relationship between the spatial arrangement of the vectors around which the variable rotations are performed and the corresponding *iso-n* contours. This finding is of importance, as topological properties and/or behavior of helical structures may be partially interpreted on the basis of such geometrical criteria.

REFERENCES

1 T. MIYAZAWA, *J. Polym. Sci.*, 55 (1961) 215–231.
2 H. SUGETA AND T. MIYAZAWA, *Biopolymers*, 5 (1967) 673–679.
3 H. SUGETA AND T. MIYAZAWA, *Biopolymers*, 6 (1968) 1387–1388.
4 R. D. FRASER AND T. P. MACRAE, *Conformation in Fibrous Proteins*, Academic Press, New York and London, 1973, pp. 134–135.
5 D. W. JONES, *J. Polym. Sci.*, 32 (1958) 371–394.
6 P. R. SUNDARARAJAN AND R. H. MARCHESSAULT, *Can. J. Chem.*, 53 (1975) 3563–3566.
7 B. K. SATHYANARAYANA AND V. S. R. RAO, *Biopolymers*, 10 (1971) 1605–1615.
8 B. K. SATHYANARAYANA AND V. S. R. RAO, *Biopolymers*, 11 (1972) 1379–1394.
9 I. TVAROSKA, S. PÉREZ, AND R. H. MARCHESSAULT, *Carbohydr. Res.*, 61 (1978) 97–106.
10 S. PÉREZ, Thèses d'État, Grenoble, France, 1978.
11 IUPAC–IUB Commission on Biochemical Nomenclature, *Arch. Biochem. Biophys.*, 145 (1971) 405.
12 D. GAGNAIRE, S. PÉREZ, AND V. TRAN, *Int. J. Biol. Macromolecules*, 1 (1979) 42–45.
13 P. ZUGENMAIER AND P. SARKO, *Biopolymers*, 12 (1973) 435–444.
14 P. R. SUNDARARAJAN AND R. H. MARCHESSAULT, *Can. J. Chem.*, 50 (1972) 792–794.
15 R. H. MARCHESSAULT AND S. PÉREZ, *Biopolymers*, 18 (1979) 2369–2374.
16 D. BASSIEUX, D. GAGNAIRE AND M. VIGNON, *Carbohydr. Res.*, 56 (1977) 19–33.
17 M. J. BOX, *Computer J.*, (1965) 67–77.
18 V. TRAN, Thèse 3ième Cycle, Grenoble, France, 1977.
19 T. L. HILL, *J. Chem. Phys.*, 16 (1948) 399–404.
20 S. PÉREZ AND R. H. MARCHESSAULT, *Carbohydr. Res.*, 65 (1978) 114–120.